

Electron paramagnetic resonance in a spin-1/2 Heisenberg strong-rung ladder

A. N. Ponomaryov,¹ M. Ozerov,^{1,*} L. Zviagina,¹ J. Wosnitzer,^{1,2} K. Yu. Povarov,³
F. Xiao,^{3,4,†} A. Zheludev,³ C. Landee,⁵ E. Čížmár,⁶ A. A. Zvyagin,^{7,8} and S. A. Zvyagin¹

¹*Dresden High Magnetic Field Laboratory (HLD-EMFL),*

Helmholtz-Zentrum Dresden-Rossendorf, D-01328 Dresden, Germany

²*Institut für Festkörperphysik, TU Dresden, D-01062 Dresden, Germany*

³*Neutron Scattering and Magnetism, Laboratory for Solid State Physics, ETH Zürich, Switzerland*

⁴*Clark University, Worcester, MA 01610, USA*

⁵*Clark University, 950 Main Street, Worcester, MA 01610, USA*

⁶*Institute of Physics, P.J. Šafárik University, Košice, Slovakia*

⁷*Max Planck Institute for the Physics of Complex Systems, D-01187 Dresden, Germany*

⁸*B. I. Verkin Institute for Low Temperature Physics and Engineering of
the National Academy of Science of Ukraine, Kharkov 61103, Ukraine*

(Dated: December 7, 2024)

We report on electron paramagnetic resonance (EPR) study of $\text{Cu}(\text{C}_8\text{H}_6\text{N}_2)\text{Cl}_2$, a spin-1/2 Heisenberg strong-rung ladder compound, for various crystal orientations with respect to applied magnetic field and in a broad temperature range. Below $T^* \sim 8$ K, the EPR line splits into two components, indicating the presence of a finite anisotropy due to magnetic dipolar interactions. At temperatures above T^* only a single EPR line was observed. The temperature dependence of the EPR linewidth is analyzed in the framework of a bosonization approach, suggesting that anisotropy of magnetic interactions plays a crucial role, determining the peculiar low-temperature EPR linewidth behavior.

PACS numbers: 75.10.Pq, 75.10.Jm, 75.50.Ee, 76.30.-v, 75.30.Et, 75.30.Gw, 75.40.Mg

Introduction.— Quantum spin ladders represent one of the most important paradigm models of quantum magnetism. Due to a variety of exotic strongly correlated states (including those induced by magnetic fields) and their unusual properties, quantum spin ladders continue to attract a lot of attention, being in the focus of modern condensed matter physics. Recently, these systems have been used to address a number of important topics, including, e.g., the magnon Bose-Einstein condensation (BEC) [1], Tomonaga-Luttinger liquid physics [2], etc. The anisotropy of magnetic spin-spin interactions (hereafter magnetic anisotropy) can significantly modify ground state properties and the excitation spectrum of such systems [3, 4]. The effect of the anisotropy is of particular importance for realization of a large number of physical phenomena, e.g., BEC, where the presence of the uniaxial U(1) symmetry (which corresponds to the global rotational symmetry of the bosonic field phase) is one of the most essential conditions.

Electron paramagnetic resonance (EPR) spectroscopy is traditionally recognized as one of the most sensitive tools to probe the magnetic anisotropy in solids. In particular, the theory of the low-temperature EPR in spin-1/2 Heisenberg chains was developed [5–7], allowing to explain the effect of the anisotropy on the EPR linewidth and field shift (see [7–9] and the references therein).

In contrast to spin chains, the effect of the anisotropy on EPR properties of spin ladders is less studied. Depending on the $J_{\text{leg}}/J_{\text{rung}}$ ratio (where J_{leg} and J_{rung} are the exchange interactions along legs and rungs, respectively), one can distinguish strong-leg ($J_{\text{leg}}/J_{\text{rung}} > 1$) or strong-rung ($J_{\text{leg}}/J_{\text{rung}} < 1$) ladders. It was shown

that in spin-1/2 strong-leg ladders the anisotropy determines the low-temperature EPR linewidth behavior [10]. A new approach to determine anisotropy parameters from the low-temperature EPR frequency shift in a spin-1/2 strong-rung ladder has been recently developed by Furuya et al. [11]. The theory was applied to $[\text{C}_5\text{H}_{12}\text{N}]_2\text{CuBr}_4$ (also known as BCPB or $(\text{Hpip})_2\text{CuBr}_4$), indicating a good agreement with the experimental data [12].

Here, we present results of EPR studies of another spin-1/2 strong-rung ladder, $\text{Cu}(\text{C}_8\text{H}_6\text{N}_2)\text{Cl}_2$ [hereafter $\text{Cu}(\text{Qnx})\text{Cl}_2$, where Qnx indicates quinoxaline, $\text{C}_8\text{H}_6\text{N}_2$]. We argue that the peculiar temperature dependence of the EPR linewidth [observed, in particular, in the temperature range $T^* \lesssim T \lesssim J_{\text{leg}}/k_B$ ($T^* \sim 8$ K)] is defined by the magnetic anisotropy. The EPR line splitting, observed in $\text{Cu}(\text{Qnx})\text{Cl}_2$ below T^* , is explained in terms of the magnetic dipolar interaction.

Experimental.— Series of $\text{Cu}(\text{Qnx})\text{Cl}_2$ single crystals of typically 1 mm³ size were synthesized at the ETH Zürich using slow diffusion in methanol solution, as described in Ref. [13].

The crystal structure of $\text{Cu}(\text{Qnx})\text{Cl}_2$ is shown schematically in Fig. 1. The compound belongs to the monoclinic space group $C2/m$ with unit cell parameters $a = 13.237$ Å, $b = 6.935$ Å, $c = 9.775$ Å, and $\beta = 107.88^\circ$ ($Z = 4$), measured at room temperature [14, 15]. The spin-1/2 Cu^{2+} ions (shown in red in Fig. 1) are bridged by quinoxaline molecules, forming chains along the two-fold rotation axis b . Two chains are coupled into a two-leg ladder over two Cl^- ions in each rung. From magnetic susceptibility measurements, the rung and the leg inter-

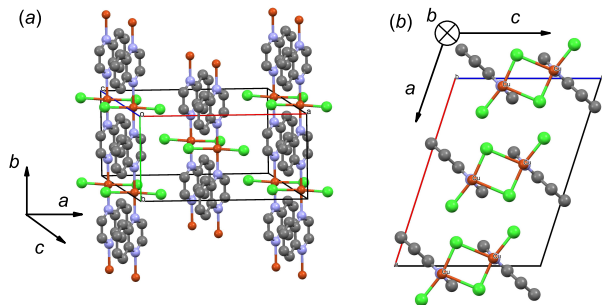


FIG. 1: (color online) Two views of the crystal structure of the spin-1/2 spin-ladder compound $\text{Cu}(\text{Qnx})\text{Cl}_2$. The Cu, N, C, and Cl ions are shown in red, blue, gray, and green, respectively. The ladders run along the b -axis direction.

actions were estimated to be 34.2 K and 18.7 K [16], respectively. Below $H_{c1} \simeq 14$ T [16], the ground state is the nonmagnetic spin singlet, while the gapped triplet is the first excited state.

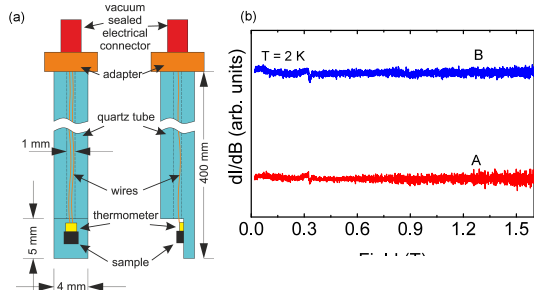


FIG. 2: (color online) (a) Schematic view of the EPR probe; (b) EPR signal of the probe without (A) and with (B) the temperature sensor. The measurements were performed at $T = 2$ K.

The EPR experiments were performed at Dresden High Magnetic Field Laboratory (Hochfeldlabor Dresden, HLD) employing the X-band “Bruker Elexsys E500” EPR spectrometer operated at a fixed frequency of 9.4 GHz. The spectrometer was equipped with the “Oxford Instruments” helium-4 flow-type cryostat with a lowest accessible temperature of ~ 2 K. In order to perform accurate temperature measurements, a special EPR probe was designed and built [schematically shown in Fig. 2(a)]. The probe was made of a quartz tube with an outer diameter of 4 mm and the inner one of 1 mm. A temperature sensor (the “LakeShore” bare chip Cernox resistor, model CX-1050-BC-HT) was installed directly next to the sample on the bottom of the probe. Temperature was measured using the “LakeShore 340” bridge. The sample was fixed using Apiezon-N vacuum grease

having direct thermal contact with the temperature sensor. The new probe was tested at lowest temperature, where parasitic contributions from the probe (including the temperature sensor) would be most pronounced. In Fig. 2(b) the signal A corresponds to the probe without the sensor (a tiny EPR signal with $g \sim 2$ from defects in the quartz tube was observed). The signal B corresponds to the probe with the sensor, showing no sign of additional EPR absorption. It is important to mention that no noticeable damping of the cavity due to the installed temperature sensor was observed.

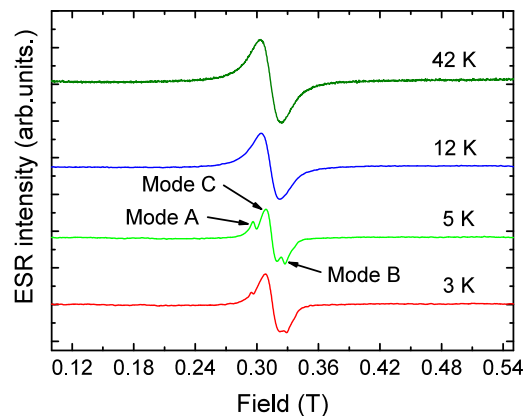


FIG. 3: (Color online) Examples of EPR spectra at temperatures above and below $T^* \sim 8$ K, measured for $H \parallel a$.

For $\text{Cu}(\text{Qnx})\text{Cl}_2$, at temperatures above $T^* \sim 8$ K, only a single resonance line was observed. The g factors, measured at room temperature, are $g_a = 2.164$, $g_b = 2.037$, and $g_c = 2.090$. Below T^* , the EPR line becomes split [Fig. 3]. Apart from the central line (mode C), two additional EPR lines, modes A and B, appear. With decreasing temperature, the modes A and B become broader and weaker, indicating transitions within the excited triplet states, until they are no longer resolved below ~ 2.5 K. Such a behavior is typical for temperature-activated exchange processes due magnetic dipole-dipole interactions [17]. In zero magnetic field, such interactions remove the degeneracy of the excited triplet, resulting in the low-temperature EPR line splitting, observed in the experiment. In the slow-exchange regime, the exchange frequency $\nu \ll g\mu_B\Delta B_{A,B}$, where $\Delta B_{A,B}$ is the difference between resonance fields for modes A and B. Here, upon raising the temperature the two lines, corresponding to the individual $\Delta M_S = 1$ transitions, get broadened and move towards each other [17]. The similar behavior was observed in another gapped spin system, $\text{BaCuSi}_2\text{O}_6$ [18]. Below 6 K, the intensity of the central mode C increases with decreasing temperature, indicating the presence of unpaired Cu^{2+} ions. We attribute this low-temperature mode to structural defects

and a tiny amount of impurities.

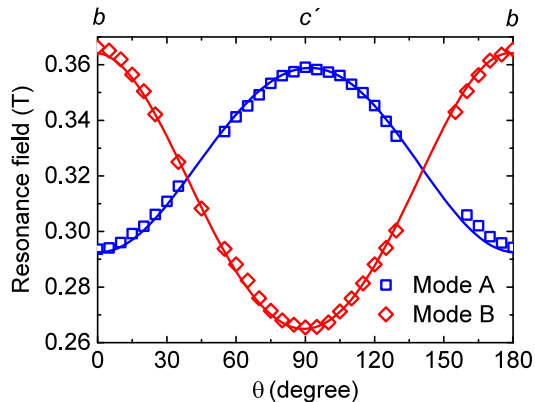


FIG. 4: (Color online) Angular dependence of the resonance positions of mode A and B (blue squares and red diamonds, respectively; $T = 5.5$ K). The solid lines represent the results, calculated with Eq. (1) using effective anisotropy parameters $D^*/k_B = 68$ mK and $E^*/k_B = 10$ mK.

Figure 4 shows the angular dependence of the resonance positions for the modes A and B with magnetic field applied in the bc' plane (the c' direction corresponds to $[001]$ axis). The rotation was performed around the a axis; the rotation angle θ was counted from $H \parallel b$. As one can clearly see, the modes have a maximum separation for $H \parallel b$ and $H \parallel c'$, while for the intermediate angles $\theta \simeq 38^\circ$ and $\theta \simeq 138^\circ$ they overlap and are not resolved.

Figure 5(a) shows the integrated intensity of the EPR absorption, measured for $H \parallel a$ down to 8 K. For comparison, the molar magnetization vs temperature measured at 0.5 T is shown in the same plot. As one can clearly see, the magnetization curve very well matches the EPR intensity data.

In Fig. 5(b), the temperature dependencies of the g factors for $H \parallel a$, $H \parallel b$, and $H \parallel c$ are shown. Our experiments reveal a noticeable change of the g factor at low temperatures, where the effects of spin-spin interactions become important.

Temperature dependences of the EPR linewidth for different orientations of magnetic field are shown in Fig. 5(c). The experiments reveal a pronounced maximum of the EPR linewidth dependence at $T \sim J/k_B$.

Discussion.— The angular dependences of the EPR positions (Fig. 4) was analyzed using the “EasySpin” simulation package [19]. Such calculations are proven to be useful for estimating effective anisotropy in spin-ladder materials using a simplified spin-triplet model for the excited state [12]. The effective spin Hamiltonian used for the simulation is

$$\mathcal{H} = \mathbf{g}\mu_B\mathbf{S}\mathbf{H} + D^*S_z^2 + E^*(S_x^2 - S_y^2), \quad (1)$$

where \mathbf{g} is the g factor tensor, μ_B is the Bohr magneton,

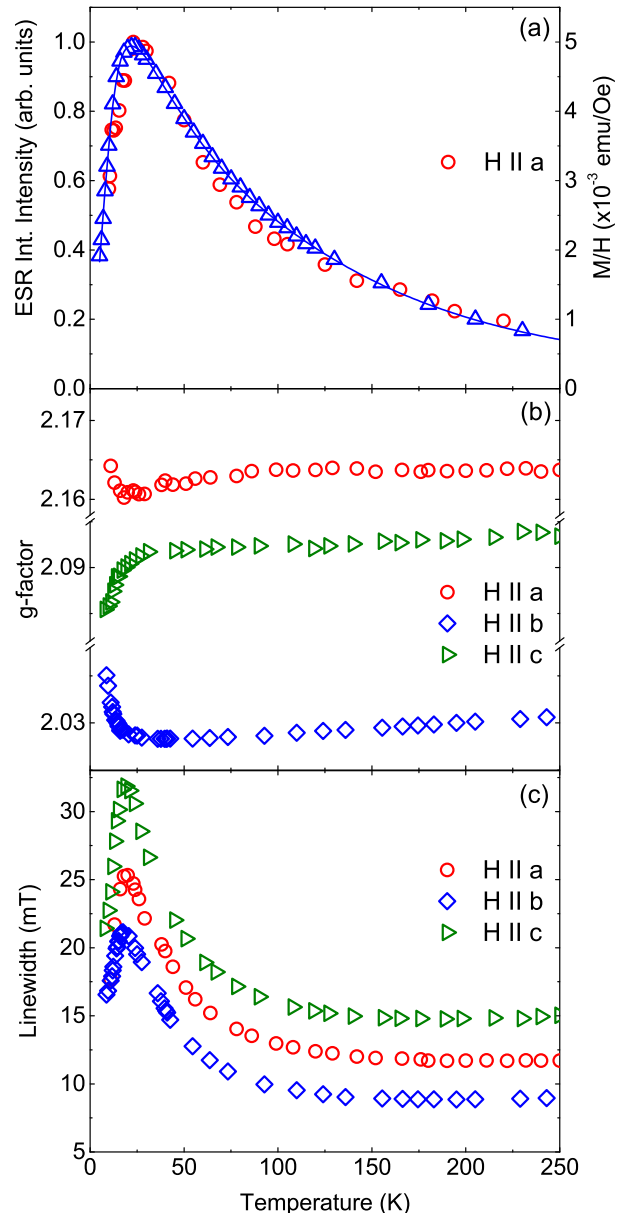


FIG. 5: (Color online) (a) Temperature dependence of the integrated EPR intensity for $H \parallel a$ (circles). The molar magnetization, measured in a magnetic field of 0.5 T (triangles; the line is guide for the eye). Temperature dependence of the g factors (b) and the EPR linewidths (c), measured for $H \parallel a$, $H \parallel b$, and $H \parallel c$ down to $T^* \sim 8$ K.

\mathbf{S} is the total spin with its projections on the corresponding axes S_x , S_y , and S_z , \mathbf{H} is the magnetic field, and D^* and E^* are the effective axial and in-plane anisotropy parameters. The results of the simulation are shown by the solid lines in Fig. 4. The best agreement of the applied model with the experimental data was found for $D^*/k_B = 68$ mK, $E^*/k_B = 10$ mK ($g_x = 2.06$, $g_y = 2.04$, and $g_z = 2.27$). On the other hand, a zero-field splitting

due to dipolar interactions can be estimated based on the distance between the Cu-ions on the rungs [20], giving $D^*/k_B \approx 50$ mK. This value is in a good agreement with our EPR estimates, suggesting that the main origin of the low-temperature EPR splitting is indeed dipolar interactions.

Now, let us discuss the EPR properties of $\text{Cu}(\text{Qnx})\text{Cl}_2$ above T^* , where other effects of the anisotropy can be relevant. As shown in Ref. [21], the Hamiltonian of the system can be reduced to an effective spin-1/2 single chain Hamiltonian. To set the stage we can describe the low-temperature behavior of the system with the Hamiltonian \mathcal{H} using the bosonization (or conformal field theory) description, namely

$$\mathcal{H} = \mathcal{H}_0 + \mathcal{H}_{\text{pert}}, \quad (2)$$

where

$$\mathcal{H}_0 = \frac{v}{2} \int dx [\Pi^2 + (\partial_x \phi)^2] \quad (3)$$

is the Hamiltonian of the free boson field ϕ and its conjugated momentum Π . The velocity of low-lying spin excitations, v , can be written as

$$v = \frac{\pi J_{\text{eff}} \sqrt{1 - \Delta^2}}{2 \arccos \Delta}. \quad (4)$$

Here, J_{eff} is the effective exchange interaction in the chain (proportional to the exchange coupling J_{leg} , [21]) and Δ is a parameter describing the uniaxial anisotropy. Notice that in the EPR experiments the real magnetic anisotropy of magnetic interactions, not the effective anisotropy of the XXZ chain for the phenomenological description of the gap in the spin ladder like in [21], matters.

The perturbation can be written as

$$\mathcal{H}_{\text{pert}} = \lambda \int dx \cos(\sqrt{8\pi K} \phi), \quad (5)$$

with the conformal field theory exponent, K , given by

$$K = \frac{\pi}{\pi - \arccos \Delta}. \quad (6)$$

The EPR intensity, $I(\omega, H, T)$, in the standard geometry can be expressed in the framework of the bosonization approach [5] for $H < J_{\text{leg}}$ (we use the units in which $\hbar = g\mu_B = k_B = 1$) as

$$I(\omega, H, T) \propto -\omega \text{Im} \frac{H^2 + \omega^2}{\omega^2 - H^2 - \Pi(\omega, H, T)}, \quad (7)$$

where ω is the frequency of the ac field and $vq = H$ (where q is the wave vector). In the above expression the self energy $\Pi(\omega, H, T)$ can be calculated in the framework of the perturbation theory with respect to λ . One can show that

$$\Pi(\omega, q) = 4\pi K v^2 \lambda^2 [F^r(\omega, q) - F^r(0, 0)], \quad (8)$$

where $F^r(\omega, q)$ is the retarded propagator of the boson field given by

$$F^r(\omega, q) \propto -\frac{2^{4K-2} v}{\pi^2 T^2} \left(\frac{\pi T}{v} \right)^{4K} \Gamma^2(1 - 2K) \times \\ \times \frac{\Gamma(K - \frac{i(\omega+vq)}{2\pi}) \Gamma(K - \frac{i(\omega-vq)}{2\pi})}{\Gamma(1 - K - \frac{i(\omega+vq)}{2\pi}) \Gamma(1 - K - \frac{i(\omega-vq)}{2\pi})},$$

where $\Gamma(x)$ is the Gamma function. In the case of resonance we have to use $\omega = H$. Then, it is clear that the shift of the resonance position due to spin-spin interactions and anisotropy is given by the real part of the self energy, while the EPR linewidth is related to its imaginary part. In particular, the linewidth, ΔB , can be expressed as

$$\Delta B \approx \lambda^2 v^2 \frac{\sqrt{\pi} K}{2^{2K}} T^{4K-3} \left(\frac{2\pi}{v} \right)^{4K-2} \times \\ \frac{\Gamma(\frac{1}{2} - K) \Gamma^2(K) \Gamma(1 - 2K)}{\Gamma(1 - K)}. \quad (9)$$

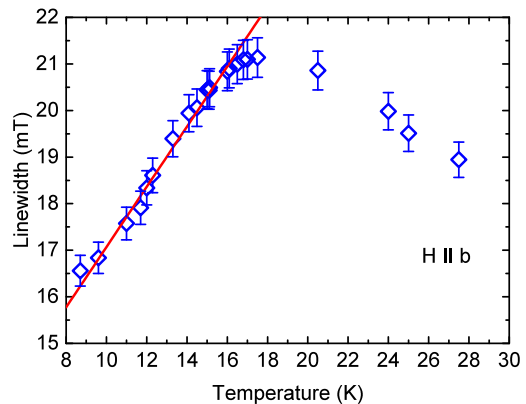


FIG. 6: (Color online) Low-temperature part of the EPR linewidth temperature dependence measured for $H \parallel b$. The line is linear fit used to find the anisotropy parameter A (see the text for details).

We can consider the weak anisotropy $A = \Delta J_{\text{eff}}$ of the system as a perturbation with respect to the isotropic antiferromagnetic case $K = 1$. Then, according to the above and neglecting corrections due to marginal perturbations, such as logarithmic ones, one finds

$$\Delta B \approx \left(\frac{A}{J_{\text{eff}}} \right)^2 T. \quad (10)$$

Such a linear dependence between ΔB and T should exist up to $T \approx J_{\text{eff}}$. Taking into account logarithmic corrections, one obtains

$$\Delta B(T) \approx A^2 \ln^2 \left(\frac{v}{T} \right) \frac{T}{v^2}. \quad (11)$$

We can estimate the anisotropy value from the EPR linewidth temperature dependence. For that we analyze the data measured for $H \parallel b$. The linear fit of the low-temperature part ($8 \lesssim T \lesssim 17$ K, Fig. 6), using the equation

$$\Delta B_{tot} = \Delta B_{TI} + \Delta B(T), \quad (12)$$

gives $\Delta B_{TI} = 11$ mT and $\Delta B(T) = kT$ ($k = 6.5$ mT/K), for the temperature-independent and temperature-dependent contributions, respectively. The first, temperature-independent contribution can be of the van Vleck origin. Accordingly to Eq. 10, the second term gives

$$A \approx \sqrt{0.0065} J_{eff} \approx 0.081 J_{eff}. \quad (13)$$

One source of EPR line broadening is the exchange anisotropy, which can be roughly estimated using the formula $D_E \approx J_{eff}(\Delta g/g)^2$ (where Δg is the deviation of the g factor from the free electron value and assuming $J_{eff} = J_{eg}$) [22], giving $D_E/k_B \sim 0.1$ K. On the other hand, it is worthwhile to mention that the uniform Dzyaloshinskii-Moriya (DM) interaction is permitted on the bonds along the ladder legs in $\text{Cu}(\text{Qnx})\text{Cl}_2$ by the symmetry. Rough estimate using formula $D_{DM} \approx J_{eff}(\Delta g/g)$ [22] gives for the DM interaction $D_{DM}/k_B \sim 1.5$ K. This value agrees well with the one obtained using Eq. 13, $A \approx 1.51$ K, suggesting that the uniform DM interaction can be the dominant source of the EPR linewidth behavior.

We can further see that for $K < 3/4$ the EPR linewidth has to decrease with increasing temperature [6], in particular, for $1/2 \leq K \leq 3/4$, which is the relevant effective interaction in the spin chain. Such a relevant perturbation is present for $\text{Cu}(\text{Qnx})\text{Cl}_2$, and can be caused, e.g., by the magnetic dipolar interaction (denoted by D^* in the effective single-spin model, see above).

In conclusion, we have presented systematic EPR studies of the spin-1/2 strong-rung Heisenberg ladder compound $\text{Cu}(\text{C}_8\text{H}_6\text{N}_2)\text{Cl}_2$. Employing the bosonization approach, we showed that the anisotropy of magnetic interactions plays a crucial role, determining the peculiar EPR linewidth behavior, observed in the experiment at low temperatures. The EPR splitting below 8 K is explained in terms of magnetic dipolar interactions, with an energy scale of less than 0.1 K.

Acknowledgments.— This work was supported by Deutsche Forschungsgemeinschaft (DFG, Germany), APVV-0132-11, and VEGA 1/0145/13. We acknowledge the support of the HLD at HZDR, member of the European Magnetic Field Laboratory (EMFL). A. A. Z. acknowledges the support from the Institute for Chemistry of V. N. Karazin Kharkov National University. Work at ETHZ was partially supported by the Swiss National Sci-

ence Foundation, Division 2. We thank M. Uhlarz for the consultations on magnetization measurements.

-
- * Present Address: FELIX Laboratory, Radboud University, 6525 ED Nijmegen, The Netherlands
 - † Present Address: Department of Physics, Durham University, Durham DH1 3LE, United Kingdom
 - [1] T. Giamarchi, C. Ruegg, and O. Tchernyshyov, *Nature Phys.* **4**, 198 (2008).
 - [2] M. Klanjšek, H. Mayaffre, C. Berthier, M. Horvatič, B. Chiari, O. Piovesana, P. Bouillot, C. Kollath, E. Orignac, R. Citro, and T. Giamarchi, *Phys. Rev. Lett.* **101**, 137207 (2008).
 - [3] O. Golinelli *et al.*, *Phys. Rev. B* **46** 10854 (1992).
 - [4] A. A. Nersesyan, A. O. Gogolin, F. H. L. Essler, *Phys. Rev. Lett.* **81**, 910 (1998).
 - [5] M. Oshikawa and I. Affleck, *Phys. Rev. Lett.* **82**, 5136 (1999).
 - [6] A. A. Zvyagin, *Phys. Rev. B* **63**, 172409 (2001).
 - [7] M. Oshikawa and I. Affleck, *Phys. Rev. B* **65**, 134410 (2002).
 - [8] S. A. Zvyagin, A. K. Kolezhuk, J. Krzystek, and R. Feynherm, *Phys. Rev. Lett.* **95**, 017207 (2005).
 - [9] A. A. Validov, M. Ozerov, J. Wosnitza, S. A. Zvyagin, M. M. Turnbull, C. P. Landee, and G. B. Teitel'baum, *J. Phys.: Condens. Matter* **26**, 026003 (2013).
 - [10] S. C. Furuya and M. Sato, *J. Phys. Soc. Jpn.* **84**, 033704 (2015).
 - [11] S. C. Furuya, P. Bouillot, C. Kollath, M. Oshikawa, and T. Giamarchi, *Phys. Rev. Lett.* **108**, 037204 (2012).
 - [12] E. Čížmár, M. Ozerov, J. Wosnitza, B. Thielemann, K. W. Krämer, C. Rüegg, O. Piovesana, M. Klanjšek, M. Horvatič, C. Berthier, and S. A. Zvyagin, *Phys. Rev. B* **82**, 054431 (2010).
 - [13] B. C. Keith, F. Xiao, C. P. Landee, M. M. Turnbull, A. Zheludev, *Polyhedron* **30**, 3006 (2011).
 - [14] J. Jorner-Somoza, N. Codina-Castillo, M. Deumal, F. Mota, J. J. Novoa, R. T. Butcher, M. M. Turnbull, C. P. Landee, J. L. Wikaira, *Inorg. Chem.* **51**, 6316, 2012.
 - [15] S. Lindroos, P. Lumme, *Acta Crystallogr., Sect. C: Cryst. Struct. Commun.* **46**, 2039 (1990).
 - [16] K. Yu. Povarov, W. E. A. Lorenz, F. Xiao, C. P. Landee, Y. Krasnikova, A. Zheludev, *J. Magnetism and Magnetic Materials*, **370**, 62 (2014).
 - [17] A. Carrington, A. D. McLachlan, *Introduction to Magnetic Resonance* (Harper and Row, New York, 1967).
 - [18] S. A. Zvyagin, J. Wosnitza, J. Krzystek, R. Stern, M. Jaime, Y. Sasago, and K. Uchinokura, *Phys. Rev. B* **73**, 094446 (2006).
 - [19] S. Stoll and A. Schweiger, *J. Magn. Reson.* **178**, 42 (2006).
 - [20] J. A. Weil and J. R. Bolton, *Electron Paramagnetic Resonance : Elementary Theory and Practical Applications* (John Wiley and Sons, Inc., Hoboken, New Jersey, 2007).
 - [21] T. Giamarchi and A. M. Tsvelik, *Phys. Rev. B* **59**, 11398 (1999).
 - [22] T. Moriya, *Phys. Rev.* **120**, 91 (1960).